Novel Organosoluble Aromatic Polyimides Bearing Pendant Methoxy-Substituted Triphenylamine Moieties: Synthesis, Electrochromic, and Gas Separation Properties

CHA-WEN CHANG,[1] HUNG-JU YEN,[2] KUAN-YEH HUANG,[3] JUI-MING YEH,[3] GUEY-SHENG LIOU[2]

[1]Department of Applied Chemistry, National Chi Nan University, 1 University Road, Puli, Nantou Hsien 54561, Taiwan

[2]Institute of Polymer Science and Engineering, National Taiwan University, Taipei 10617, Taiwan

[3]Department of Chemistry and Center for Nanotechnology and R&D Center for Membrane Technology, Chung-Yuan Christian University, Chung Li 32023, Taiwan

Received 3 August 2008; accepted 16 September 2008
DOI: 10.1002/pola.23082
Published online in Wiley InterScience (www.interscience.wiley.com).

ABSTRACT: Four series of polyimides **I–VI** with pendent triphenylamine (TPA) units having inherent viscosities of 0.44–0.88 dL/g were prepared from four diamines with two commercially available tetracarboxylic dianhydrides via a conventional two-step procedure that included a ring-opening polyaddition to give polyamic acids, followed by chemical cyclodehydration. These polymers were amorphous and could afford flexible films. All the polyimides had useful levels of thermal stability associated with high softening temperatures (279–300 °C), 10% weight-loss temperatures in excess of 505 °C, and char yields at 800 °C in nitrogen higher than 58%. The hole-transporting and electrochromic properties were examined by electrochemical and spectroelectrochemical methods. Cyclic voltammograms of the polyimide films cast onto an indium-tin oxide (ITO)-coated glass substrate exhibited a or two reversible oxidation couples at 0.65–0.78 and 1.00–1.08 V versus Ag/AgCl in acetonitrile solution. The polymer films revealed electrochromic characteristics with a color change from neutral pale yellowish to blue doped form at applied potentials ranging from 0.00 to 1.20 V. The CO_2 permeability coefficients (P_{CO_2}) and permeability selectivity (P_{CO_2}/P_{CH_4}) for these polyimide membranes were in the range of 4.73–16.82 barrer and 9.49–51.13, respectively. J Polym Sci Part A: Polym Chem 46: 7937–7949, 2008
Keywords: electrochemistry; functionalization of polymers; gas permeation; high-performance polymers; polyimides; polycondensation

INTRODUCTION

Electrochromism is known as the reversible change of the color resulting from the oxidation or the reduction of the material by electrochemical means. Color changes are commonly between a transparent state, where the chromophore only absorbs in the UV region, and a colored state or between two colored states in a given electrolyte solution. The electrochromic material may exhibit several colors and be termed polyelectrochromic. This interesting property led to the development of many technological applications such as automatic antiglazing mirror,[1] smart windows,[2] electrochromic displays,[3] and chameleon materials.[4]

Correspondence to: G.-S. Liou (E-mail: gsliou@ntu.edu.tw) or J.-M. Yeh (E-mail: juiming@cycu.edu.tw)

Journal of Polymer Science: Part A: Polymer Chemistry, Vol. 46, 7937–7949 (2008)

Triphenylamine (TPA)-containing polymers[5] are not only widely used as electrochromic materials,[6] but also show interesting behavior of gas separation.[7] Among the various classes of polymers,[8] polyimides are widely studied[9] for use in gas separation because of its inherent advantages such as good gas transport properties, thermal and chemical stability, as well as mechanical property.[10] Polyimides derived from 2,2-bis(3,4-dicarboxyphenyl)hexafluoropropane dianhydride (6FDA) exhibit high gas permeability and permselectivity of CO_2/CH_4 separation, which is attributed to the presence of bulky —$C(CF_3)_2$— moiety that hinders intrasegmental mobility and disrupts interchain packing and stiffens the backbones.[11–16] In addition to the favorable gas transport properties, fluorine-containing polyimides also possess excellent thermal and mechanical characteristics.[17–19] However, the technological applications of most polyimides are limited by processing difficulties because of high melting or glass transition temperatures and limited solubility in most organic solvents because of their rigid backbones. To overcome these limitations, polymer-structure modification becomes necessary. One of the common approaches for increasing solubility and processability of polyimides without sacrificing high thermal stability is the introduction of bulky, packing disruptive TPA groups into the polymer backbone.[20] Recently, we have reported the synthesis of soluble aromatic polyimides bearing TPA units in the main chain based on *N,N*-bis(4-aminophenyl)-*N′,N′*-diphenyl-1,2-phenylenediamine[21] and 4,4′-diamino-4′′-*N*-carbazolytriphenylamine, respectively.[22] Because of the incorporation of bulky, propeller-shaped TPA units along the polymer backbone, all the polymers were amorphous, soluble in many aprotic solvents with good film-forming capability, and had excellent thermal stability.

The electrochemistry of TPA in aprotic solvents has been well studied.[23] The TPA cationic radical of the first electron oxidation is not stable, chemical reaction therefore follows to produce tetraphenylbenzidine by tail-to-tail (para-positions) coupling with the loss of two protons per dimer. When the phenyl groups were incorporated by electron-donating substituents at the para position of TPA, the coupling reactions were greatly prevented by affording stable cationic radicals thus enhancing the electrochromic characteristic.[24,25] The research aim about gas separation was placed in understanding the relationships between the gas permeability, permselectivity, and the polymer composition by adjusting different TPA-containing diamine structures in 6FDA-based polyimides. In this article, to obtain processable polyimide materials with multifunctions such as good electrochromic and gas separation property, we therefore synthesized four series of polyimides bearing TPA groups from four different diamines, 4,4′-diaminotriphenylamine (**1**), 4,4′-diamino-4"-methoxytriphenylamine (**2**), *N,N*-bis(4-aminophenyl)-*N′,N′*-diphenyl-1,4-phenylenediamine (**3**), and *N,N*-bis(4-aminophenyl)-*N′,N′*-di(4-methoxyphenyl)-1,4-phenylenediamine (**4**). The general properties such as solubility, crystallinity, and thermal properties are described. The electrochemical, electrochromic, and gas permeation properties of these polymers are also investigated herein and are compared with each other.

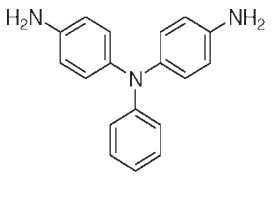

1

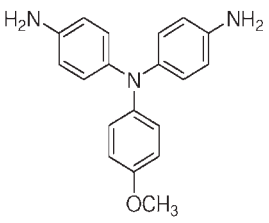

2

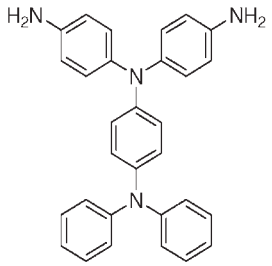

3

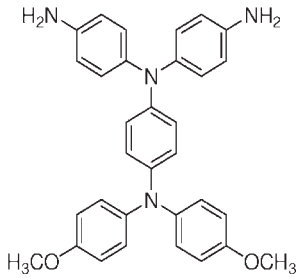

4

EXPERIMENTAL

Materials

4,4′-Diaminotriphenylamine[26] (**1**) (mp: 186–187 °C), 4,4′-diamino-4"-methoxytriphenylamine[27,28] (**2**) (mp: 150–152 °C), *N,N*-bis(4-aminophenyl)-*N′,N′*-diphenyl-1,4-phenylenediamine[21] (**3**) (mp: 245–247 °C), and *N,N*-bis(4-aminophenyl)-*N′,N′*-di(4-methoxyphenyl)-1,4-phenylenediamine[29] (**4**) (mp: 87–89 °C) were synthesized from cesium fluoride- or sodium hydride-assisted nucleophilic displacement reaction of 4-fluoronitrobezene with aniline, *p*-anisidine, 4-aminotriphenylamine, and 4-amino-4′,4′′-dimethoxytriphenylamine, respectively, followed by hydrazine Pd/C-catalyzed

reduction. Commercially available aromatic tetracarboxylic dianhydrides such as 3,3′,4,4′-diphenylsulfonetetracarboxylic dianhydride (DSDA; **5a**; Tokyo Chemical Industry Co., Ltd. (TCI)) were purified by recrystallization from acetic anhydride. 2,2-Bis(3,4-dicarboxyphenyl)hexafluoropropane dianhydride (6FDA; **5b**; Chriskev) was purified by vacuum sublimation. Tetrabutylammonium perchlorate (TBAP; ACROS) were recrystallized twice by ethyl acetate under nitrogen atmosphere and then dried *in vacuo* prior to use. All other reagents were used as received from commercial sources.

Preparation of Polyimides by Two-Step Method

The synthesis of polyimide **IIa** was used as an example to illustrate the general synthetic route. To a solution of 0.3817 g (1.25 mmol) of diamine **2** in 9.5 mL of *N*-methyl-2-pyrrolidinone (NMP), 0.4478 g (1.25 mmol) of dianhydride DSDA (**5a**) was added in one portion. The mixture was stirred at room temperature overnight (∼12 h) to afford a viscous poly(amic acid) solution. The poly (amic acid) was subsequently converted to polyimide **IIa** via a chemical imidization process by addition of pyridine 2 mL and acetic anhydride 5 mL, and then the mixture was heated at 100 °C for 2 h to effect complete imidization. The resulting polymer solution was poured into 300 mL of methanol giving a fibrous precipitate, which was washed thoroughly with methanol and collected by filtration. The precipitate was dissolved in 8 mL of *N*,*N*-dimethylacetamide (DMAc), and the homogeneous solution was poured into a 9-cm glass culture dish, which was placed in a 90 °C oven for 12 h to remove the solvent. Then the obtained film was further dried *in vacuo* at 180 °C for 6 h. The inherent viscosity of polyimide **IIa** was 0.44 dL/g in NMP at a concentration of 0.5 g/dL at 30 °C.

^{1}H NMR (300 MHz, DMSO-d_6, δ, ppm): 3.73 (s, 3H, OCH_3), 6.96 (d, 4H, H_c), 7.08 (d, 4H, H_b), 7.13 (d, 2H, H_d), 7.29 (d, 4H, H_a), 8.16 (d, 2H, H_g), 8.59 (d, 2H, H_f), 8.62 (s, 2H, H_e).

Measurements

Infrared spectra were recorded on a Perkin–Elmer RXI FT-IR spectrometer. Elemental analyses were run on a Elementar Vario EL-III. ^{1}H spectra were measured on a Bruker AV-300 FT-NMR system. The inherent viscosities were determined at 0.5 g/dL concentration using a Tamson TV-2000 viscometer at 30 °C. Gel permeation chromatographic (GPC) analysis was performed on a Lab Alliance RI2000 instrument (one column, MIXED-D from Polymer Laboratories) connected with one refractive index detector from Schambeck SFD Gmbh. All GPC analyses were performed using a polymer/*N*,*N*-dimethylformamide (DMF) solution at a flow rate of 1 mL/min at 70 °C and calibrated with polystyrene standards. Wide-angle X-ray diffraction (WAXD) measurements were performed at room temperature (∼25 °C) on a Shimadzu XRD-7000 X-ray diffractometer (40 kV, 20 mA), using graphite-monochromatized Cu Kα radiation. Ultraviolet–visible (UV–vis) spectra of the polymers were recorded on a Varian Cary 50 Probe spectrometer. Thermogravimetric analysis (TGA) was conducted with a Perkin-Elmer Pyris 1 TGA. Experiments were carried out on ∼6–8 mg film samples heated in flowing nitrogen or air (flow rate = 30 cm^3/min) at a heating rate of 20 °C/min. Differential scanning calorimetry (DSC) analyses were performed on a Perkin–Elmer Pyris Diamond DSC at a scan rate of 20 °C/min in flowing nitrogen (20 cm^3/min). Thermomechanical analysis (TMA) was conducted with a Perkin–Elmer TMA 7 instrument. The TMA experiments were conducted from 50 to 350 °C at a scan rate of 10 °C/min, with a penetration probe 1.0 mm in diameter under an applied constant load of 50 mN. Softening temperatures (T_s) were taken as the onset temperatures of probe displacement on the TMA traces. Cyclic voltammetry was performed with a Bioanalytical System model CV-27 potentiostat, and a BAS X-Y recorder with indium tin oxide (ITO; polymer films area about 0.7 cm ×0.7 cm) was used as a working electrode and a platinum wire as an auxiliary electrode at a scan rate of 50 mV/s against a Ag/AgCl reference electrode in a solution of 0.1 M TBAP/acetonitrile (CH_3CN). Voltammograms are presented with the positive potential pointing to the left and with increasing anodic currents pointing downwards. The spectroelectrochemical cell was composed of a 1-cm cuvette, ITO as a working electrode, a platinum wire as an auxiliary electrode, and an Ag/AgCl reference electrode. Absorption spectra in spectroelectrochemical analysis were measured with a HP 8453 UV–visible spectrophotometer. Photoluminescence (PL) spectra were measured with a Jasco FP-6300 spectrofluorometer. All corrected fluorescence excitation spectra were found to be equivalent to their respective absorption spectra. Gas permeability for the polymer membranes with about

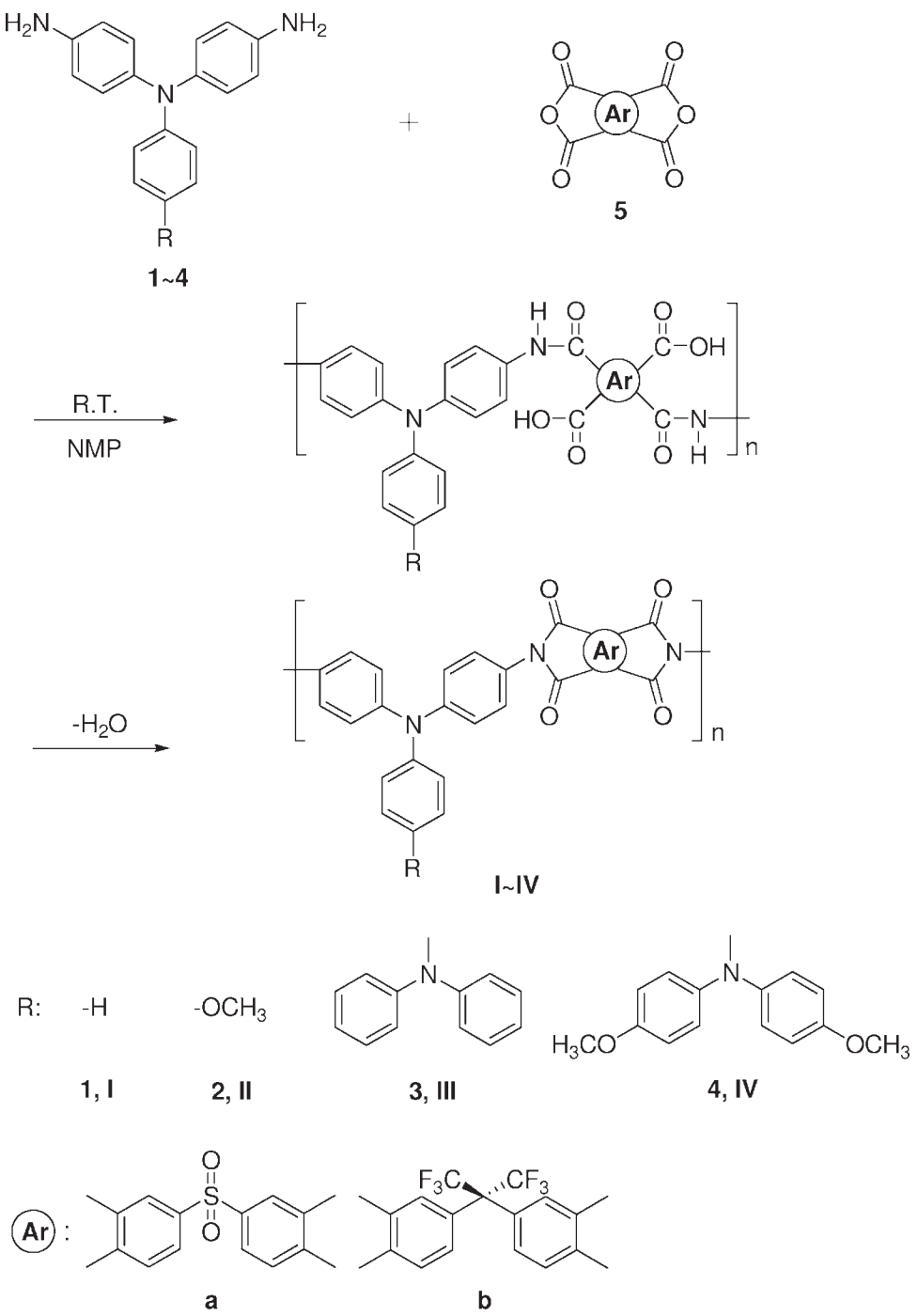

Scheme 1. Synthesis of polyimides by two-step method via chemical imidization reaction.

95–135 μm of thickness were measured with a GTR-10 model gas permeability analyzer (Yanagimoto Co., Kyoto, Japan), which consists of upstream and downstream parts separated by a membrane. Gases measured include O_2, N_2, CO_2, and CH_4. The pressure on one face of the free-standing film (or called membrane) was kept at 294 kPa, and the other face was at zero pressure initially to allow the gas to permeate through the free-standing film. The rate of transmission of gas was obtained by gas chromatography, from which the gas permeability was calculated.

Table 1. Inherent Viscosities and GPC Data of Polyimides

Polymer	η_{inh}[a] (dL/g)	M_w[b]	M_n[b]	PDI
Ia	0.50	58,000	41,000	1.39
Ib	0.48	77,000	52,000	1.49
IIa	0.44	58,000	43,000	1.34
IIb	0.88	189,000	137,000	1.39
IIIa	0.72	64,000	46,000	1.40
IIIb	0.63	112,000	82,000	1.36
IVa	0.64	80,000	55,000	1.47
IVb	0.59	116,000	89,000	1.31

[a] Measured at a polymer concentration of 0.5 g/dL in NMP at 30 °C.
[b] Relative to polystyrene standards, using DMF as the eluant.

RESULTS AND DISCUSSION

Polymer Synthesis

Four series of polyimides **I–IV** bearing pendant TPA units were prepared by the reaction of diamine **1–4** with two commercially available dianhydrides **5a** and **5b** in NMP at room temperature to form the precursor poly(amic acid)s, followed by chemical imidization (Scheme 1). In the first step, the viscosities of the reaction mixtures became very high as poly(amic acid)s were formed, indicating the formation of high-molecular-weight polymers. The poly(amic acid) precursors could be chemically dehydrated to polyimides by treatment with acetic anhydride and pyridine, and could afford flexible and tough films. The inherent viscosities and GPC analysis data of these polyimides are summarized in Table 1, and the formation of polyimides was confirmed with IR and NMR spectroscopy. The IR spectra of these polymers exhibited characteristic imide absorption bands at around 1781 (symmetrical C=O), 1723 (symmetrical C=O), 1381 (C—N), and 740 cm^{-1} (imide ring deformation). The microstructures of these polyimides were also verified by the high-resolution NMR spectra (Fig. 1).

Polymer Properties

Basic Characterization

The color of polyimide films depends markedly on the chemical structure of the dianhydride components. The obtained polyimide **I–IV** films were from yellowish to deep reddish or brownish that could be attributed to charge-transfer complex

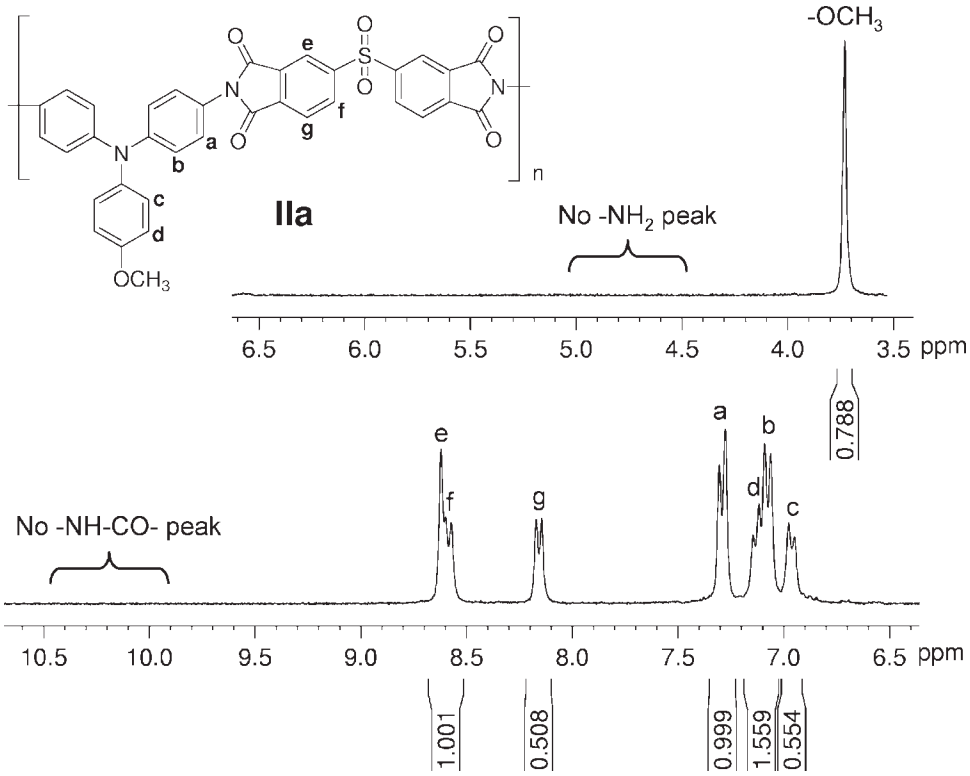

Figure 1. ^{1}H NMR spectrum of polyimide **IIa** in DMSO-d_6.

Table 2. Solubility[a] of Polyimides

	Solvents						
Polymer	NMP	DMAc	DMF	DMSO	*m*-Cresol	THF	$CHCl_3$
Ia	++	++	++	+	+	−	±
Ib	++	++	++	+	+	++	++
IIa	++	++	++	+	++	−	±
IIb	++	++	++	+	++	++	++
IIIa	++	++	++	+	+	++	++
IIIb	++	++	++	+	+	++	++
IVa	++	++	++	++	++	++	++
IVb	++	++	++	+	+	++	++

++, Soluble at room temperature; +, soluble on heating; ±, partially soluble; −, insoluble even on heating; DMSO, dimethyl sulfoxide.

[a] Qualitative solubility was tested with 1 mg of a sample in 1 mL of stirred solvent.

(CTC) formation between the electron-donating TPA unit and the strongly electron-accepting phthalimide unit. The WAXD studies of the poly (amine-imide)s indicated that all the polymers were essentially amorphous. The amorphous nature can be attributed to the introduction of bulky, twisted, three-dimensional TPA units along the polymer backbone. The solubility behavior of polymers **I–IV** obtained by chemical imidization was investigated qualitatively, and the results are listed in Table 2. The solubility behavior of the polyimides depended on their chain packing ability and intermolecular interactions that was affected by the rigidity, symmetry, and regularity of the molecular backbone. These polyimides **I–IV** exhibited higher solubility in polar aprotic organic solvents such as NMP, DMAc, DMF, and *m*-cresol. The polyimides **Ib–IVb** were soluble not only in polar aprotic organic solvents but also in less polar solvents such as THF and $CHCl_3$. The excellent solubility can be attributable to the existence of the hexafluoroisopropylidene structure that limits the CTC formation and reduce the intermolecular interactions. The thermal properties of these polyimides are summarized in Table 3. Typical TGA curves for polyimide **IIIb** and **IVb** are reproduced in Figure 2. All of the polyimides exhibited a similar TGA pattern with no significant weight loss below 500 °C in air or nitrogen atmosphere. The 10% weight-loss temperatures of the polymers in nitrogen and air were recorded in the range of 505–600 °C and 515–600 °C, respectively. The polyimides prepared from fluorine-based tetracarboxylic dianhydrides (**5b**) exhibited

Table 3. Thermal Properties of Polyimides

			T_d at 5% Weight Loss[c] (°C)		T_d at 10% Weight Loss[c] (°C)		Char Yield[d] (wt %)
Polymer	T_g[a] (°C)	T_s[b] (°C)	N_2	Air	N_2	Air	N_2
Ia	306	300	500	520	540	570	59
Ib	299	290	570	560	600	590	64
IIa	304	296	490	485	515	515	58
IIb	308	297	540	525	580	565	60
IIIa	303	287	525	545	575	600	65
IIIb	290	285	560	555	590	585	67
IVa	292	279	475	490	505	520	62
IVb	285	283	505	500	550	560	61

[a] Midpoint temperature of the baseline shift on the second DSC heating trace (rate = 20 °C/min) of the sample after quenching from 400 to 50 °C (rate = 100 °C/min) in nitrogen.

[b] Softening temperature measured by TMA with a constant applied load of 50 mN at a heating rate of 10 °C/min.

[c] Decomposition temperature, recorded via TGA at a heating rate of 20 °C/min and a gas-flow rate of 30 cm^3/min.

[d] Residual weight percentage at 800 °C in nitrogen.

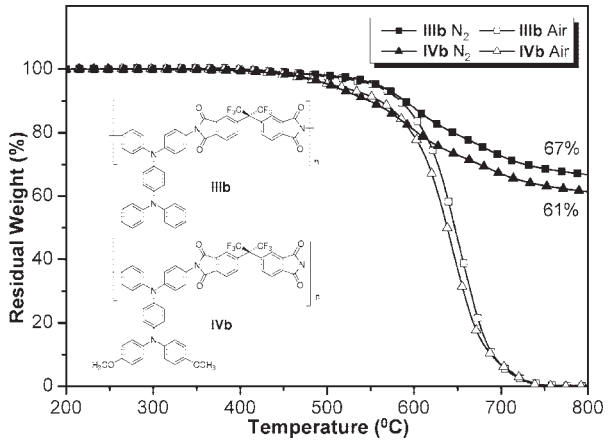

Figure 2. TGA thermograms of polyimides **IIIb** and **IVb** at a scan rate of 20 °C/min.

higher T_d values than its analogous sulfone-based tetracarboxylic dianhydrides (**5a**), and this increase may be a result of stronger C—F bonding of the CF_3 groups. The amount of carbonized residue (char yield) of these polymers in nitrogen atmosphere was more than 58% at 800 °C. The high char yields of these polymers can be ascribed to their high aromatic content. The softening temperatures (T_s) determined from the onset temperature of the probe displacement on the TMA trace of all the polymers were observed in the range of 279–300 °C.

Optical and Electrochemical Properties

The optical and electrochemical properties of these polymers were investigated by UV–vis and PL spectroscopy and cyclic voltammetry. The results are summarized in Table 4. The organosoluble polyimides **I–IV** exhibited UV–vis absorption bands, with λ_{max} at 299–307 nm in NMP solutions and 300–306 nm in films that was similar to those in the solution state, assignable to the π-π^* transition resulting from the conjugation between the aromatic rings and nitrogen atoms that combines the characteristic π-π^* transitions of TPA moieties. These TPA-based polyimides exhibited a weak fluorescence emission maximum at around 392–431 nm in the NMP solution. The cutoff wavelengths (absorption edge; λ_0) from the UV–vis transmittance spectra are also included in Table 4. It revealed that most of the visible region can be absorbed by polyimides **Ia–IVa**, which showed higher λ_0 values. This is consistent with the results that these polyimide films appeared red brown to deep-brown color. In contrast, the polyimides **Ib–IVb** showed a light color and high optical transparency, with a cutoff wavelength in the range of 505–543 nm because of lower capability of intermolecular CTC formation (as shown in Fig. 3).

The electrochemical behavior of the polyimides **I–IV** series was investigated by cyclic

Table 4. Optical and Electrochemical Properties of Polyimides

	λ in Solution (nm)[a]		λ in Film (nm)			Oxidation/V (vs. Ag/AgCl in CH_3CN) First		Second		HOMO[e] (eV)	LUMO[f] (eV)
Index	Abs Max	PL Max[b]	λ_0[c]	Abs Max	Abs Onset	$E_{1/2}$	E_{onset}	$E_{1/2}$	E_g[d] (eV)	E_{onset}	E_{onset}
Ia	304	412	562	304	567	1.04	0.97	–[g]	2.19	5.33	3.14
Ib	302	397	505	302	544	1.07	0.98	–	2.28	5.34	3.06
IIa	299	403	598	300	558	0.96	0.81	–	2.22	5.17	2.95
IIb	299	392	518	300	570	0.96	0.86	–	2.18	5.22	3.04
IIIa	307	431	600	306	544	0.77	0.68	1.13	2.28	5.04	2.76
IIIb	306	399	532	303	553	0.78	0.70	1.13	2.24	5.06	2.82
IVa	305	414	637	304	584	0.65	0.56	1.00	2.12	4.92	2.80
IVb	303	410	543	301	594	0.68	0.56	1.00	2.09	4.92	2.83

[a] Polymer concentration of 10^{-4} M in NMP at room temperature.
[b] They are excited at the abs_{max} for both the solid and solution states.
[c] The cutoff wavelength from the UV–vis transmission spectra of polymer films.
[d] The data were calculated by the equation: gap = $1240/\lambda_{onset}$ of polymer film.
[e] The HOMO energy levels were calculated from cyclic voltammetry and were referenced to ferrocene (4.8 eV).
[f] LUMO = HOMO $-E_g$.
[g] –, No discernible oxidation was observed.

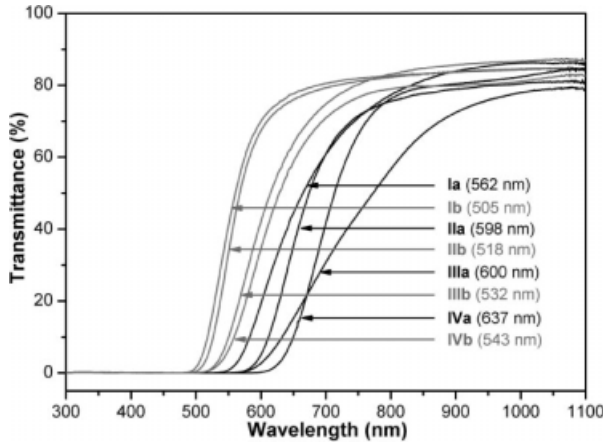

Figure 3. UV–vis transmission spectra of polyimides **I–IV** series films (thickness: 80–130 μm).

voltammetry conducted by film cast on an ITO-coated glass substrate as the working electrode in dry acetonitrile (CH_3CN) containing 0.1 M of TBAP as an electrolyte under nitrogen atmosphere. The typical cyclic voltammograms for polyimide **IVa** (with 4,4′-dimethoxy-substituted) and **IIIa** (without 4,4′-dimethoxy-substituted) are shown in Figure 4 for comparison. There are two reversible oxidation redox couples at $E_{1/2}$ values of 0.65 (E_{onset} = 0.56) and 1.01 V for polyimide **IVa**, and 0.77 (E_{onset} = 0.68) and 1.13 V for polyimide **IIIa** in the oxidative scan. Because of the electrochemical stability and good adhesion between the polyimide film and ITO substrate, polyimide **IVa** exhibited reversibility of electrochromic characteristics in 30 continuous cyclic scans between 0.0 and 1.20 V, changing the color from colorless to green and then blue at electrode potentials ranging over 0.65 and 1.01 V. Comparing the electrochemical data, we found that polyimides **IV** (with 4-methoxy-substituted) was much more easily oxidized than polyimides **III** (without 4-methoxy-substituted), and the first electron removal for polyimides **IV** was assumed to occur at the N atom on the pendant 4,4′-dimethoxytriphenylamine unit, which was more electron-richer than the N atom on the main chain TPA unit.[30,31] The introduction of electron-donating 4,4′-dimethoxytriphenylamine moieties not only greatly prevent the coupling reaction but also lower the oxidation potentials of the electroactive polyimides **IV** when compared with the corresponding polyimides **III**. Similar tendencies were observed with polyimide **I** and **II**; that is, polyimide **II** was much more easily oxidized than polyimide **I**. The energy of the highest occupied molecular orbital (HOMO) and lowest unoccupied molecular orbital (LUMO) levels of the investigated polyimides could be determined from the oxidation onset potentials and the onset absorption wavelength of polymer films, and the results are listed in Table 4. For example (Fig. 4), the oxidation onset potential for polyimide **IVa** was determined to be 0.56 V versus Ag/AgCl. The external ferrocene/ferrocenium (Fc/Fc^+) redox standard $E_{1/2}$ (Fc/Fc^+) was 0.44 V versus Ag/AgCl in CH_3CN. Under the assumption that the HOMO energy for the ferrocene standard was 4.80 eV with respect to the zero vacuum level, the HOMO energy for polyimide **IVa** was evaluated to be 4.92 eV.

Electrochromic Characterization

Electrochromism of the polyimide thin films was examined by an optically transparent thin-layer electrode coupled with UV–vis spectroscopy. The electrode preparations and solution conditions were identical to those used in cyclic voltammetry. All these polymers exhibited similar electrochromic properties, and the typical electrochromic transmittance spectra of polyimide **IVa** is shown in Figure 5. Figure 6 shows the three-dimensional % transmittance-wavelength-applied potential correlations of this sample. The peak of transmittance at 306 nm, characteristic for neutral form polyimide **IVa**, decreased gradually when the applied potentials increased positively from 0 to 0.90 V, and two new bands grew up at 418 and 986 nm because of the first stage oxidation. When the potential was adjusted to a more positive

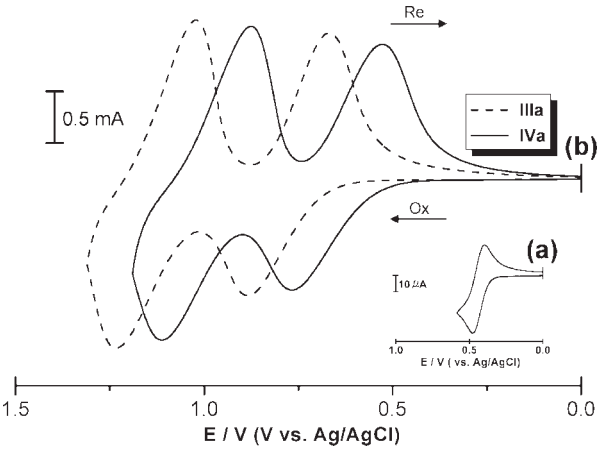

Figure 4. Cyclic voltammograms of polyimides **IIIa** and **IVa** film onto an indium-tin oxide (ITO)-coated glass substrate in CH_3CN containing 0.1 M TBAP. Scan rate = 0.05 V/s. (a) ferrocene, (b) first and second oxidation redoxs of poly(amine-imide)s **IIIa** and **IVa**.

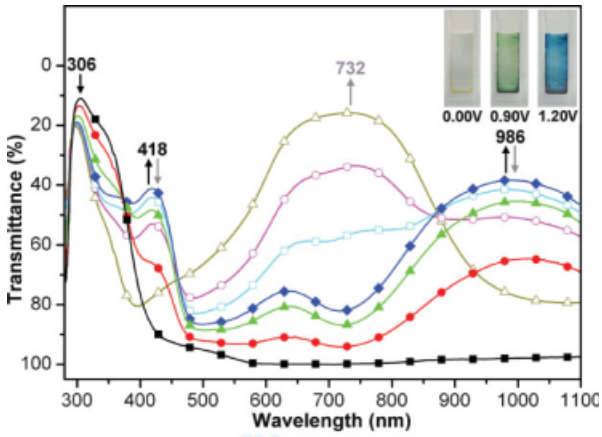

Figure 5. Electrochromic behavior of polyimide **IVa** thin film (in CH_3CN with 0.1 M TBAP As the supporting electrolyte) at 0.00 (■), 0.70 (●), 0.80 (▲), 0.90 (◆), 1.00 (□), 1.10 (○), and 1.20 (△) (V versus Ag/AgCl). $\mathbf{IVa}^{+\bullet}$: (solid symbol with black solid arrow); $\mathbf{IVa}^{2+}$: (hollow symbol with gray solid arrow).

value of 1.20 V, corresponding to the second-step oxidation, the peak of characteristic absorbance decreased gradually and one new band grew up at 732 nm. Meanwhile, the film changed from original colorless to green and then to a blue oxidized form. Polyimide **IVa** exhibited high contrast of optical transmittance change ($\Delta T\%$) up to 60% at 986 nm for green and 84% at 732 nm for blue.

The color-switching times were estimated by applying a potential step, and the absorbance profiles were followed (Figs. 7 and 8) for polymer

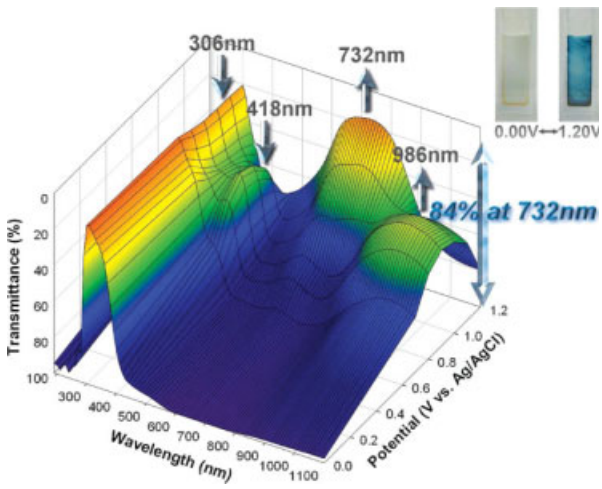

Figure 6. 3-D spectroelectrochemical behavior of the **IVa** thin film on the ITO-coated glass substrate (in CH_3CN with 0.1 M TBAP as the supporting electrolyte) from 0 to 1.2 V (versus Ag/AgCl).

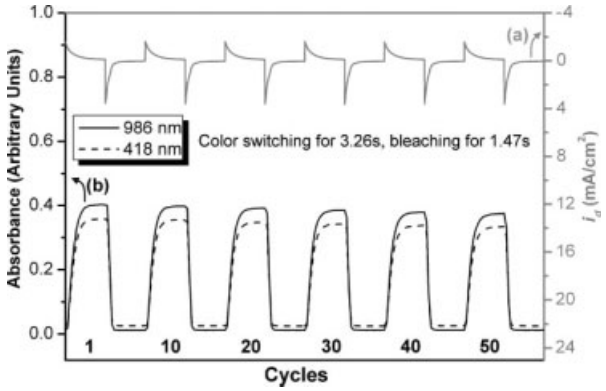

Figure 7. (a) Current consumption and (b) potential step absorptometry of polyimide **IVa** (in CH_3CN with 0.1 M TBAP as the supporting electrolyte) by applying a potential step (0.00 V ⇄ 0.80 V), (coated area: 1 cm^2) and cycle time 18 s for coloration efficiency from 118 cm^2/C (1st cycle) to 110 cm^2/C (50th cycle).

IVa. The switching time was defined as the time required for reach 90% of the full change in absorbance after the switching of the potential. Thin film of polyimide **IVa** required 3.26 s at 0.80 V for switching absorbance at 418 and 986 nm and 1.47 s for bleaching. When the potential was set at 1.18 V, thin film **IVa** required 4.22 s for coloration at 732 nm and 1.42 s for bleaching. After over 30 cyclic scans, the polymer film still exhibited stability of electrochromic characteristics. The electrochromic coloration efficiency of green ($\eta = \Delta OD_{986}/Q$) (118 cm^2/C for 1 cycle to 110 cm^2/C for 50 cycles), and blue ($\eta = \Delta OD_{732}/Q$) (123 cm^2/C for 1 cycle to 110 cm^2/C for 30 cycles) and decay of

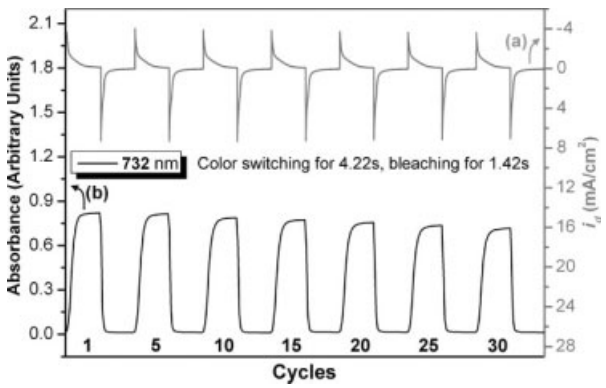

Figure 8. (a) Current consumption and (b) potential step absorptometry of polyimide **IVa** (in CH_3CN with 0.1 M TBAP as the supporting electrolyte) by applying a potential step (0.00 V ⇄ 1.18 V), (coated area: 1 cm^2) and cycle time 24 s for coloration efficiency from 123 cm^2/C (1st cycle) to 110 cm^2/C (30th cycle).

Table 5. Optical and Electrochemical Data Collected for Polyimide **IVa** Coloration Efficiency Measurements

Cycles[a]	ΔOD_{986}[b]		Q[c] (mC/cm^2)		η[d] (cm^2/C)		Decay[e] (%)	
1	0.391	(0.834)[f]	3.31	(6.77)	118	(123)	0	(0)
10	0.386	(0.776)	3.37	(6.67)	115	(116)	2.5	(4.1)
20	0.380	(0.742)	3.36	(6.52)	113	(114)	4.2	(6.5)
30	0.374	(0.703)	3.34	(6.37)	112	(110)	5.1	(10.6)
40	0.367	—[g]	3.33	—	110	—	6.8	—
50	0.363	—	3.29	—	110	—	6.8	—

[a] Times of cyclic scan by applying potential steps: 0.00 ↔ 0.80, 0.00 ↔ 1.18 for parenthesis (V vs. Ag/AgCl).
[b] Optical density change at 986 nm.
[c] Ejected charge, determined from the *in situ* experiments.
[d] Coloration efficiency is derived from the equation: $\eta = \Delta OD/Q$.
[e] Decay of coloration efficiency after cyclic scans.
[f] Data in parentheses are optical density change at 732 nm.
[g] The poly(amine-imide) is not measured after 30 cycles.

the polyimide **IVa** were also calculated,[32] and the results are summarized in Table 5.

Gas Separation

Gas permeability measurements were carried out for polyimides **I–IV** membranes with about 95–135 μm of thickness. The gas permeability was measured by the following equation:

$$P = l/(p_1 - p_2) \times \frac{q/t}{A}$$

where P is the gas permeability [cm^3(STP) cm/cm^2 s cmHg], q/t is the volumetric flow rate of the gas permeate [cm^3(STP)/s], l is the free-standing film thickness (cm), A is the effective free-standing film area (cm^2), and p_1 and p_2 are the pressures (cmHg) on the high-pressure and low-pressure sides of the freestanding film, respectively. Table 6 summarizes the gas permeability coefficients of the polymer membranes. It is clear that the permeabilities of polyimides correlate with their structures. The oxygen permeability coefficients (P_{O_2}) of **IIb** with 4-methoxy-substituted was 4.28 barrer, which was higher than that of **Ib** (P_{O_2} : 0.69) without 4-methoxy-substituted. Similar tendencies were observed with other polymers; that is, polymer **IVb** was more permeable to gases than was polymer **IIIb**. The separation factors (α), based on ratios of pure gas permeability coefficients, are presented for O_2/N_2 and CO_2/CH_4 pairs in Table 6. Increasing in permeability is generally known to be accompanied by decrease in permselectivity, which is consistent with the well-known permeability/selectivity tradeoff rule common in strongly size-sieving polymers. Robeson[33] demonstrated an upper bound in double logarithmic plots of selectivity against permeability for a wide range of polymers. Robeson plots (double logarithmic plots) of selectivity versus permeability are shown in Figure 9 for O_2/N_2 and CO_2/CH_4. Chemically, the —C(CF$_3$)$_2$— group disrupts and redirects the phenyl groups in polymer chains with the bulky fluorine atoms and the sp^3 carbon

Table 6. Permeability Coefficients and Ideal Separation Factors Measured at 35 °C and 1 atm

	Permeation Permeabilities[a] (Barrer)				Permselectivities ($\alpha_{A/B}$)	
Index	P_{O_2}	P_{N_2}	P_{CO_2}	P_{CH_4}	P_{O_2}/P_{N_2}	P_{CO_2}/P_{CH_4}
Ib	0.69	0.08	4.73	0.08	8.63	59.13
IIb	4.28	0.89	16.82	0.50	4.81	33.64
IIIb	1.97	0.45	11.77	1.24	5.05	9.49
IVb	2.94	0.59	12.97	0.40	4.98	32.43

[a] Permeability values are given in units of barrers, where 1 barrer = 10^{-10} cm^3 (STP) cm/(cm^2 s cmHg), (thickness: 95–135 μm).

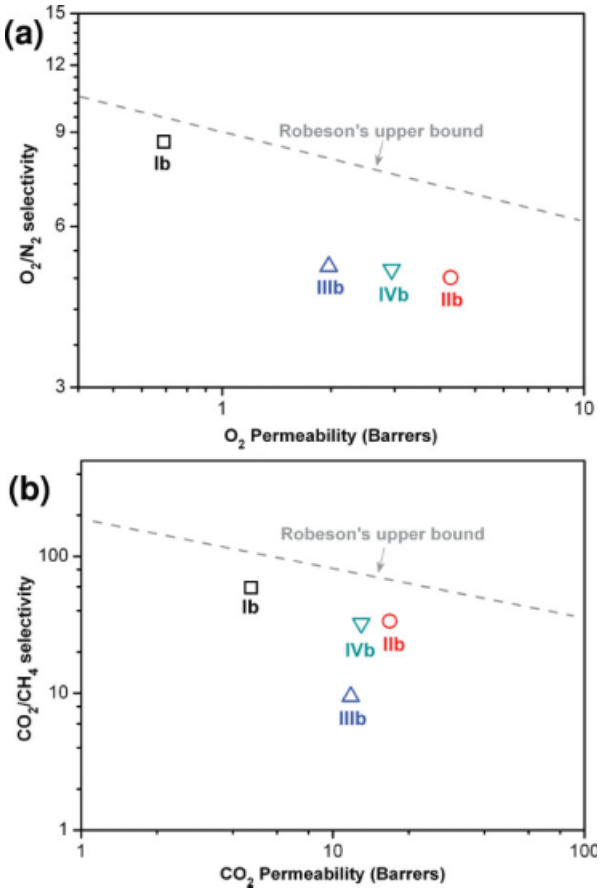

Figure 9. Double-logarithmic plots of (a) O_2/N_2 selectivity versus O_2 permeability and (b) CO_2/CH_4 selectivity versus CO_2 permeability for permeable polyimides. [Color figure can be viewed in the online issue, which is available at www.interscience.wiley.com.]

linking the two phenyl rings in 6FDA. Because of the sp^3 carbon, these flat two phenyl rings form a 109.5° angle between their respective centers, while the phenyl rings occupy different molecular planes. Thus, the polyimides **Ib**, **IIb**, and **IVb** membranes exhibited higher selectivity for CO_2/CH_4 separation because of the presence of bulky —$C(CF_3)_2$— group that hinders intrasegmental mobility and disrupts interchain packing and stiffens the backbones.

CONCLUSIONS

Four series of polyimides were readily prepared by the two-step method starting from diamines **1–4** with two commercial tetracarboxylic dianhydrides. All the polyimides were amorphous with high T_s and exhibited excellent thermal stability. The polyimide films showed good adherent behavior and were found to be electroactive, and also revealed electrochromic characteristics, changing color from the original pale yellowish neutral form to green and then to a blue oxidized form when scanning potentials positively from 0.00 to 1.20 V. Polymer **IVa** showed excellent continuous cyclic stability of electrochromic characteristic with good coloration efficiency of green (118 cm^2/C for 1 cycle to 110 cm^2/C for 50 cycles) and blue (123 cm^2/C for 1 cycle to 110 cm^2/C for 30 cycles). After over 30 cyclic switches, the polymer films still exhibited stability of electrochromic characteristics. Thus, the 4-methoxy-substituted TPA-based polyimides could be good candidates as anodic electrochromic materials because of their proper oxidation potentials, electrochemical stability, and thin film formability. Gas transport properties of these polyimides for CO_2, CH_4, O_2, and N_2 have been investigated. It is shown that the introduction of the bulky TPA unit into aromatic polyimides can improve gas transport properties by increasing permeability, with only minor decreases in permselectivity. The combination of electrochromic and gas permeable properties along with excellent thermal stability makes these new polyimides as newly processable high-performance polymers with multifunction.

The authors are grateful to the National Science Council of the Republic of China for its financial support of this work.

REFERENCES AND NOTES

1. Byker, H. J. (Gentex Corp.). U.S. Patent 4,902,108, Feb. 20, 1990.
2. Mortimer, R. G. Chem Soc Rev 1997, 26, 147–156.
3. (a) Monk, P. M. S. J. Electroanal Chem 1997, 432, 175–179; (b) Monk, P. M. S. In Handbook of Luminescence, Display Materials and Devices, Nalwa, H. S.; Rohwer, L. S., Eds.; American Scientific, 2003; Vol 3, pp 261–370.
4. (a) Meeker, D. L.; Mudigonda, D. S. K.; Osborn, J. M.; Loveday, D. C.; Ferraris, J. P. Macromolecules 1998, 31, 2943–2946; (b) Mudigonda, D. S. K.; Meeker, D. L.; Loveday, D. C.; Osborn, J. M.; Ferraris, J. P. Polymer 1999, 40, 3407–3412; (c) Brotherston, I. D.; Modigonda, D. S. K.; Osborn, J. M.; Belk, J.; Chen, J.; Loveday, D. C.; Boehme, J. L.; Ferraris, J. P.; Meeker, D. L. Electrochim Acta 1999, 44, 2993–3004.
5. (a) Liou, G. S.; Yen, H. J. J Polym Sci Part A: Polym Chem 2006, 44, 6094–6102; (b) Liou, G. S.; Lin, H. Y.; Hsieh, Y. L.; Yang, Y. L. J Polym Sci

Part A: Polym Chem 2007, 45, 4921–4932; (c) Kuo, C. H.; Cheng, W. K.; Lin, K. R.; Leung, M. K.; Hsieh, K. H. J Polym Sci Part A: Polym Chem 2007, 45, 4504–4513; (d) Huo, L.; He, C.; Han, M.; Zhou, E.; Li, Y. J Polym Sci Part A: Polym Chem 2007, 45, 3861–3871; (e) Lee, S. K.; Ahn, T.; Cho, N. S.; Lee, J. I.; Jung, Y. K.; Lee, J.; Shim, H. K. J Polym Sci Part A: Polym Chem 2007, 45, 1199–1209; (f) Liou, G. S.; Huang, N. K.; Yang, Y. L. J Polym Sci Part A: Polym Chem 2007, 45, 48–58; (g) Liou, G. S.; Huang, H. M.; Hsiao, S. H.; Chang, C. W.; Yen, H. J. J Polym Res 2007, 14, 191–199; (h) Lin, H. Y.; Liou, G. S.; Lee, W. Y.; Chen, W. C. J Polym Sci Part A: Polym Chem 2007, 45, 1727–1736; (i) Liou, G. S.; Lin, S. M.; Yen, H. J. Eur Polym J 2008, 44, 2608–2618.

6. (a) Ogino, K.; Kanagae, A.; Yamaguchi, R.; Sato, H.; Kurtaja, J. Macromol Rapid Commun 1999, 20, 103–106; (b) Yu, W. L.; Pei, J.; Huang, W.; Heeger, A. J. Chem Commun 2000, 8, 681–682; (c) Chou, M. Y.; Leung, M. K.; Su, Y. O.; Chiang, S. L.; Lin, C. C.; Liu, J. H.; Kuo, C. K.; Mou, C. Y. Chem Mater 2001, 16, 654–661; (d) Liou, G. S.; Chen, H. W.; Yen, H. J. J Polym Sci Part A: Polym Chem 2006, 44, 4108–4121; (e) Liou, G. S.; Yang, Y. L.; Chen, W. C.; Su, Y. O. J Polym Sci Part A: Polym Chem 2007, 45, 3292–3302; (f) Liou, G. S.; Chang, C. W.; Huang, H. M.; Hsiao, S. H. J Polym Sci Part A: Polym Chem 2007, 45, 2004–2014; (g) Hsiao, S. H.; Liou, G. S.; Kung, Y. C.; Yen, H. J. Macromolecules 2008, 41, 2800–2808.
7. Li, W.; Li, S.; Zhang, Q.; Zhang, S. Macromolecules 2007, 40, 8205–8211.
8. (a) Dai, Y.; Guiver, M. D.; Robertson, G. P.; Kang, Y. S. Macromolecules 2005, 38, 9670–9678; (b) Hu, C. C.; Fu, Y. J.; Hsiao, S. W.; Lee, K. R.; Lai, J. Y. J Membr Sci 2007, 303, 29–36; (c) Hu, C. C.; Liu, T. C.; Lee, K. R.; Ruaan, R. C.; Lai, J. Y. Desalination 2006, 193, 14–24; (d) Yeh, J. M.; Chen, C. L.; Chen, Y. C.; Ma, C. Y.; Huang, H. Y.; Yu, Y. H. J Appl Polym Sci 2004, 92, 631–637.
9. (a) Li, W.; Chen, G.; Zhang, S.; Wang, H.; Yan, D. J Polym Sci Part A: Polym Chem 2007, 45, 3550–3561; (b) Ye, Y. S.; Yen, Y. C.; Chen, W. Y.; Cheng, C. C.; Chang, F. C. J Polym Sci Part A: Polym Chem 2008, 46, 6296–6304; (c) Liu, J. G.; Nakamura, Y.; Shibasaki, Y.; Ando, S.; Ueda, M. J Polym Sci Part A: Polym Chem 2007, 45, 5606–5617; (d) Lin, C. H.; Lin, C. H. J Polym Sci Part A: Polym Chem 2007, 45, 2897–2912; (e) Liaw, D. J.; Wang, K. L.; Chang, F. C.; Lee, K. R.; Lai, J. Y. J Polym Sci Part A: Polym Chem 2007, 45, 2367–2374; (f) Miyatake, K.; Yasuda, T.; Hirai, M.; Nanasawa, M.; Watanabe, M. J Polym Sci Part A: Polym Chem 2007, 45, 157–163.
10. (a) Guiver, M. D.; Robertson, G. P.; Dai, Y.; Bilodeau, F.; Kang, Y. S.; Lee, K. J.; Jho, J. Y.; Won, J. O. J.; Polym Sci Part A: Polym Chem 2002, 40, 4193–4204; (b) Ayala, D.; Lozano, A. E.; de Abajo, J.; Garćia-Perez, C.; de la Campaa, J. G.; Peinemann, K. V.; Freeman, B. D.; Prabhakar, R. J Membr Sci 2003, 215, 61–73; (c) Stern, S. A. J Membr Sci 1994, 94, 1–65; (d) Mi, Y.; Stern, S. A. Trohalaki, S. J Membr Sci 1993, 77, 41–48; (e) Matsumoto, K.; Xu, P. J Membr Sci 1993, 81, 23–29; (f) Yeh, J. M.; Hsieh, C. F.; Jaw, J. H.; Kuo, T. H.; Huang, H. Y.; Lin, C. L.; Hsu, M. Y. J Appl Polym Sci 2005, 95, 1082–1090; (g) Ghanem, B. S.; McKeown, N. B.; Budd, P. M.; Selbie, J. D.; Fritsch, D. Adv Mater 2008, 20, 2766–2771.
11. Koros, W. J.; Fleming, G. K.; Jordan, S. M.; Kim, T. H.; Hoehn, H. H. Prog Polym Sci 1988, 13, 339–401.
12. Kim, T. H.; Koros, W. J.; Husk, G. R.; O'Brien, K. C. J Membr Sci 1988, 37, 45–62.
13. Liu, Y.; Wang, R.; Chung, T. S. J Membr Sci 2001, 189, 231–239.
14. Liu, Y.; Chung, T. S.; Wang, R.; Li, D. F.; Chng, M. L. Ind Eng Chem Res 2003, 42, 1190–1195.
15. Ren, J.; Wang, R.; Chung, T. S.; Li, D. F.; Liu, Y. J Membr Sci 2003, 222, 133–147.
16. Coleman, M. R.; Koros, W. J. J Polym Sci Part B: Polym Phys 1994, 32, 1915–1926.
17. Stern, S. A.; Mi, Y.; Yamamoto, H.; St Clair, A. K. J Polym Sci Part B: Polym Phys 1989, 27, 1887–1909.
18. Coleman, M. R.; Koros, W. J. Macromolecules 1999, 32, 3106–3113.
19. Cao, C.; Chung, T. S.; Liu, Y.; Wang, R.; Pramoda, K. P. J Membr Sci 2003, 216, 257–268.
20. (a) Imai, Y. High Perform Polym 1995, 7, 337–345; (b) Imai, Y. React Funct Polym 1996, 30, 3–15; (c) Hsiao, S. H.; Li, C. T.; Macromolecules 1998, 31, 7213–7217; (d) Liou, G. S. J Polym Sci Part A: Polym Chem 1998, 36, 1937–1943; (e) Eastmond, G. C.; Paprotny, J.; Irwin, R. S. Polymer 1999, 40, 469–486; (f) Eastmond, G. C.; Gibas, M.; Paprotny, J. Eur Polym J 1999, 35, 2097–2106; (g) Reddy, D. S.; Chou, C. H.; Shu, C. F.; Lee, G. H. Polymer 2003, 44, 557–563; (h) Myung, B. Y.; Ahn, C. J.; Yoon, T. H. Polymer 2004, 45, 3185–3193.
21. Cheng, S. H.; Hsiao S. H. Su, T. H.; Liou, G. S. Macromolecules 2005, 38, 307–316.
22. Liou, G. S.; Hsiao, S. H.; Chen, H. W. J Mater Chem 2006, 16, 1831–1842.
23. Seo, E. T.; Nelson, R. F.; Fritsch, J. M.; Marcoux, L. S.; Leedy, D. W.; Adams, R. N. J Am Chem Soc 1966, 88, 3498–3503.
24. Hagopian, L.; Kohler, G.; Walter, R. I. J Phys Chem 1967, 71, 2290–2296.
25. Ito, A.; Ino, H.; Tanaka, K.; Kanemoto, K.; Kato, T. J Org Chem 2002, 67, 491–498.
26. Oishi, Y.; Ishida, M.; Kakimoto, M.; Imai, Y.; Kurosaki, T. J Polym Sci Part A: Polym Chem 1992, 30, 1027–1035.

27. Nishikata, Y.; Fukui, S.; Kakimoto, M.; Imai, Y.; Nishiyama, K.; Fujihira, M. Thin Solid Films 1992, 296, 210–211.
28. Chiu, K. Y.; Su, T. X.; Li, J. H.; Lin, T. H.; Liou, G. S.; Cheng, S. H. J Electroanal Chem 2005, 575, 95–101.
29. Liou, G. S.; Chang, C. W. Macromolecules 2008, 41, 1667–1674.
30. Su, T. H.; Hsiao, S. H.; Liou, G. S. J Polym Sci Part A: Polym Chem 2005, 43, 2085–2098.
31. Nelson, R. F.; Adams, R. N. J Am Chem Soc 1968, 90, 3925–3930.
32. Mortimer, R. J.; Reynolds, J. R. J Mater Chem 2005, 15, 2226–2233.
33. (a) Robeson, L. M. J Membr Sci 1991, 62, 165–185; (b) Robeson, L. M. Curr Opin Solid State Mater Sci 1999, 4, 549–552; (c) Robeson, L. M.; Borgoyne, W. F.; Langsam, M.; Savoca, A. C.; Tien, C. F. Polymer 1994, 35, 4970–4978.

DOI 10.1002/pola